STABILITY OF OFFSHORE STRUCTURES IN SHALLOW WATER DEPTH

F. Van den Abeele[1] and J. Vande Voorde[1]

[1] OCAS N.V., J.F. Kennedylaan 3, 9060 Zelzate, Belgium

Abstract

The worldwide demand for energy, and in particular fossil fuels, keeps pushing the boundaries of offshore engineering. Oil and gas majors are conducting their exploration and production activities in remote locations and water depths exceeding 3000 meters. Such challenging conditions call for enhanced engineering techniques to cope with the risks of collapse, fatigue and pressure containment.

On the other hand, offshore structures in shallow water depth (up to 100 meter) require a different and dedicated approach. Such structures are less prone to unstable collapse, but are often subjected to higher flow velocities, induced by both tides and waves. In this paper, numerical tools and utilities to study the stability of offshore structures in shallow water depth are reviewed, and three case studies are provided.

First, the Coupled Eulerian Lagrangian (CEL) approach is demonstrated to combine the effects of fluid flow on the structural response of offshore structures. This approach is used to predict fluid flow around submersible platforms and jack-up rigs.

Then, a Computational Fluid Dynamics (CFD) analysis is performed to calculate the turbulent Von Karman street in the wake of subsea structures. At higher Reynolds numbers, this turbulent flow can give rise to vortex shedding and hence cyclic loading. Fluid structure interaction is applied to investigate the dynamics of submarine risers, and evaluate the susceptibility of vortex induced vibrations.

As a third case study, a hydrodynamic analysis is conducted to assess the combined effects of steady current and oscillatory wave-induced flow on submerged structures. At the end of this paper, such an analysis is performed to calculate drag, lift and inertia forces on partially buried subsea pipelines.

Keywords fluid structure interaction, multiphysics, offshore structures, wave loads, stability, design

1 INTRODUCTION: DESIGN CONSIDERATIONS FOR OFFSHORE STRUCTURES

Offshore structures like oil and gas platforms, drilling rigs, semi-submersibles and jack-up barges have to withstand complex, combined loading patterns during their entire design life. The anticipated loads include the dead weight of the structure, hydrostatic pressure and any imposed forces. In addition, the structure has to cope with environmental loading, including wind and wave action combined with sometimes strong tidal flows. The main design considerations for such offshore structures are structural redundancy, corrosion resistance and fatigue life, especially for welded nodal joints.

The implications on material selection are shown on Figure 1. For topsides, deck structures and module walls, which are only subjected to wind loading and dead weight, secondary structural steels (like S275) can be used. Cranes and modules supports, which require a higher level of structural integrity, are typically made out of quenched and tempered steel grades like S420. Jack-up legs are tubular sections made out of primary structural steels, whereas steel piles will typically be quenched and tempered grades. Welded nodal joints require special attention, as they are prone to fatigue damage. For such critical components, special structural steels are often required.

During normal operations, the offshore structure will be subjected to waves loading and tidal flows. In addition, the part of the structure above the sea water level is exposed to wind loading. Moreover, the wind contributes to the current velocity at the still water level as well. This contribution can be estimated as

$$W = W_0 \frac{d_0 + z}{d_0} \quad \left(-d_0 \le z \le 0\right) \qquad \text{(Eq. 01)}$$

with W_0 the wind-generated current velocity at the still water level and d_0 the reference depth.

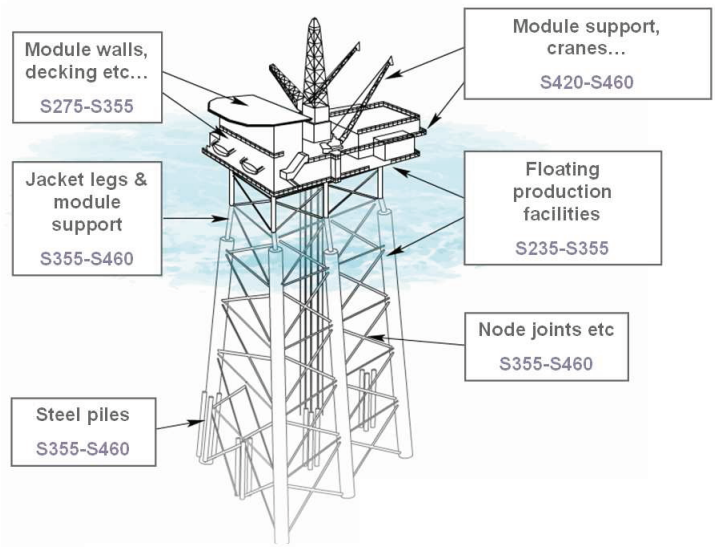

Figure 1: Material selection for offshore structures

Currents induce time-constant water particle velocities, although they normally vary along the spatial coordinates. Current velocity as a function of depth is commonly estimated by a one-seventh power law

$$V(z) = V_0 \left[\frac{d+z}{d} \right]^{1/7} \quad (z \le 0) \qquad \text{(Eq. 02)}$$

where d is the water depth and V_0 is the tidal current at the still water level. In shallow waters, the current induced velocity can generate a significant load on the structure. Differences in (measured) tidal height δH can be converted to expected current velocity V by the Voith relation

$$V = m(\delta H)^n \qquad \text{(Eq. 03)}$$

where *m* is a scaling factor and *n* the shape exponent. A prediction of current velocity is shown on Figure 2, indicating that the fluid flow velocity in shallow water can range between V = 1 m/s to V = 5 m/s.

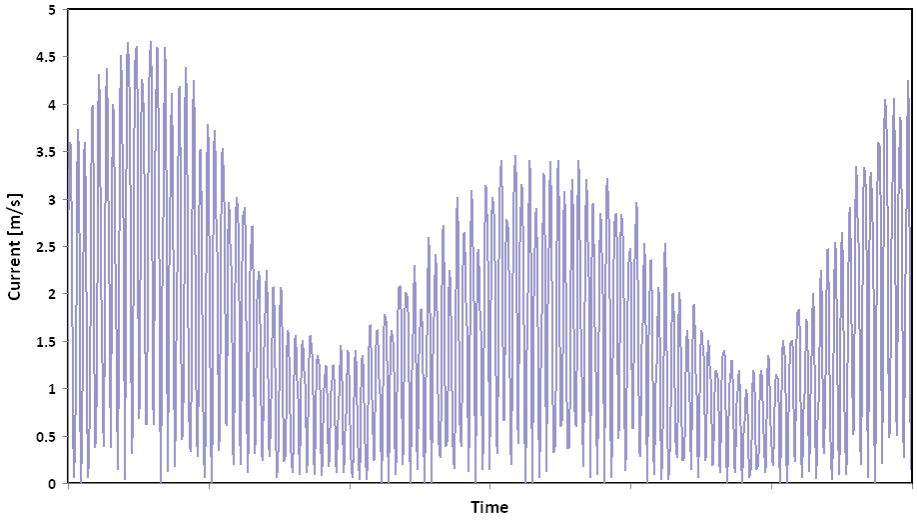

Figure 2: Fluid flow velocity induced by tidal flow

A sea state consists not only of currents, but also of waves. In reality, there is always a steady current underlying waves. Based on the water depth d and the (measured) wave period T, the corresponding wave length can be calculated with Airy wave theory [1] by iteratively solving the transcendent equation

$$L = \frac{gT^2}{2\pi} \tanh\left(\frac{2\pi d}{L} \right) \qquad \text{(Eq. 04)}$$

A wave with wave length L, height H and period T in a water depth d induces a horizontal water particle velocity

$$u_x = \frac{\pi H}{T} \frac{\cosh\{2\pi(z+d)/L\}}{\sinh\{2\pi d/L\}} \cos\left\{2\pi\left(\frac{x}{L} - \frac{t}{T}\right)\right\} \quad \text{(Eq. 05)}$$

which gives rise to a drag and a lift force, and the corresponding acceleration

$$a_x = \frac{2\pi^2 H}{T^2} \frac{\cosh\{2\pi(z+d)/L\}}{\sinh\{2\pi d/L\}} \sin\left\{2\pi\left(\frac{x}{L} - \frac{t}{T}\right)\right\} \quad \text{(Eq. 06)}$$

will induce an inertia force. When designing offshore structures in shallow water, the water depth is generally (much) smaller than the wave length:

$$d < \frac{L}{20} \quad \text{(Eq. 07)}$$

and the wave length (Eq. 04) can be approximated by

$$L \approx T\sqrt{g\,d} \quad \text{(Eq. 08)}$$

and the simplified equations for velocity (Eq. 06) and acceleration (Eq. 07) read

$$\begin{cases} u_x \approx \dfrac{\pi H}{k\,d\,T} \cos\theta \\ a_x \approx \dfrac{2\pi^2 H}{k\,d\,T^2} \sin\theta \end{cases} \quad \text{(Eq. 09)}$$

with $k = 2\pi/L$ the wave number and $\theta = 2\pi\left(\frac{x}{L} - \frac{t}{T}\right)$ the phase angle.

In this paper, three case studies are presented for which the shallow water approximation (Eq. 07) holds. First, the Coupled Eulerian Lagrangian approach is demonstrated to predict the response of a jack-up barge subjected to wave loading and strong tidal flows. Then, a Computational Fluid Dynamics (CFD) analysis is performed to calculate the turbulent Von Karman street in the wake of subsea structures. As a third case study, a hydrodynamic analysis is conducted to assess the combined effects of steady current and oscillatory wave-induced flow and the drag, lift and inertia forces exerted on partially buried subsea pipelines.

2 COUPLED EULERIAN LAGRANGIAN APPROACH TO SIMULATE JACK-UP RIGS

Jack-up barges are floating vessels with long legs that can be raised or lowered. The jack-up barge is towed onto location with its legs in the upright position, and the barge floating on the water surface. Once arrived at location, the legs are jacked down onto the seabed. Jack-up barges can be used as drilling rigs or service vessels (e.g. to install offshore windmills or to decommission obsolete production platforms), and typically operate in shallow water depth.

In Figure 3, a typical jack-up barge is shown, where the accommodation and deck structure is supported by four tubular legs. With a leg length of up to 100 meters, a diameter of 3 meters and a wall thickness of 50 mm, jack-up barges are slender structures which are susceptible to the effects of hydrodynamic loading.

To predict the response of a jack-up barge subjected to wave loading and strong tidal flows, fluid structure interaction (FSI) is required. To enable full coupling between the fluid flow and the structural response, a general purpose finite element code has to be coupled with a CFD solver, which is a tedious and expensive operation when contact conditions are complex. The Coupled Eulerian Lagrangian (CEL) approach, demonstrated here, allows the fluid and structural solution to proceed in a single framework, without constraints on the mesh motion or the topology of the fluid-structure interface.

Figure 3: Jack-up barge supported by four tubular legs

For structural mechanics simulations, the Lagrangian formulation is commonly used, in which the nodes move with the underlying material. This formulation makes it easy to track the free surfaces of a material, but may result in extensive mesh distortion when strain gradients are high. To minimize mesh distortion, the arbitrary Lagrangian Eulerian (ALE) adaptive meshing technique can be used, where the mesh motion is constrained to the material motion at the free boundaries only. For analyses with more extreme deformations, such as fluid flow, the Eulerian technique may be the only method that can provide a solution. In an Eulerian formulation, the nodes stay fixed, while the material flows through the mesh. Although this approach makes it more difficult to track the material boundaries, it has the distinct advantage of completely eliminating mesh distortion due to material deformation.

To simulate the response of a jack-up barge to tidal flows and wave loading, a Coupled Eulerian Lagrangian (CEL) approach is followed. In a CEL analysis, an Eulerian mesh (the fluid flow domain) and a Lagrangian mesh (the jack-up barge, modelled as compliant structure) are assembled in the same model, and interactions between the two meshes are enforced using general contact.

The structural response of the Lagrangian parts is calculated by applying the principle of virtual work [2]

$$\int_V \rho u_i \, \delta u_i \, dV + \int_V \sigma_{ij} \, \delta \varepsilon_{ij} \, dV - \int_V f_i \, \delta u_i \, dV = \int_S \sigma_{ij} \, n_j \, \delta u_i \, dS \qquad \text{(Eq. 09)}$$

where S is the boundary of the Lagrangian body V, σ_{ij} are the stress components, ε_{ij} the strain components, f_i the external forces and u_i the unknown displacements. To model the jack-up barge, a rigid deck structure with a mass M = 3000 tonnes is assumed. The 50 meter long legs are modelled as perfectly plastic steel tubulars (with a yield stress σ_y = 355 MPa) with a diameter D = 2.5 m and a wall thickness t = 50 mm.

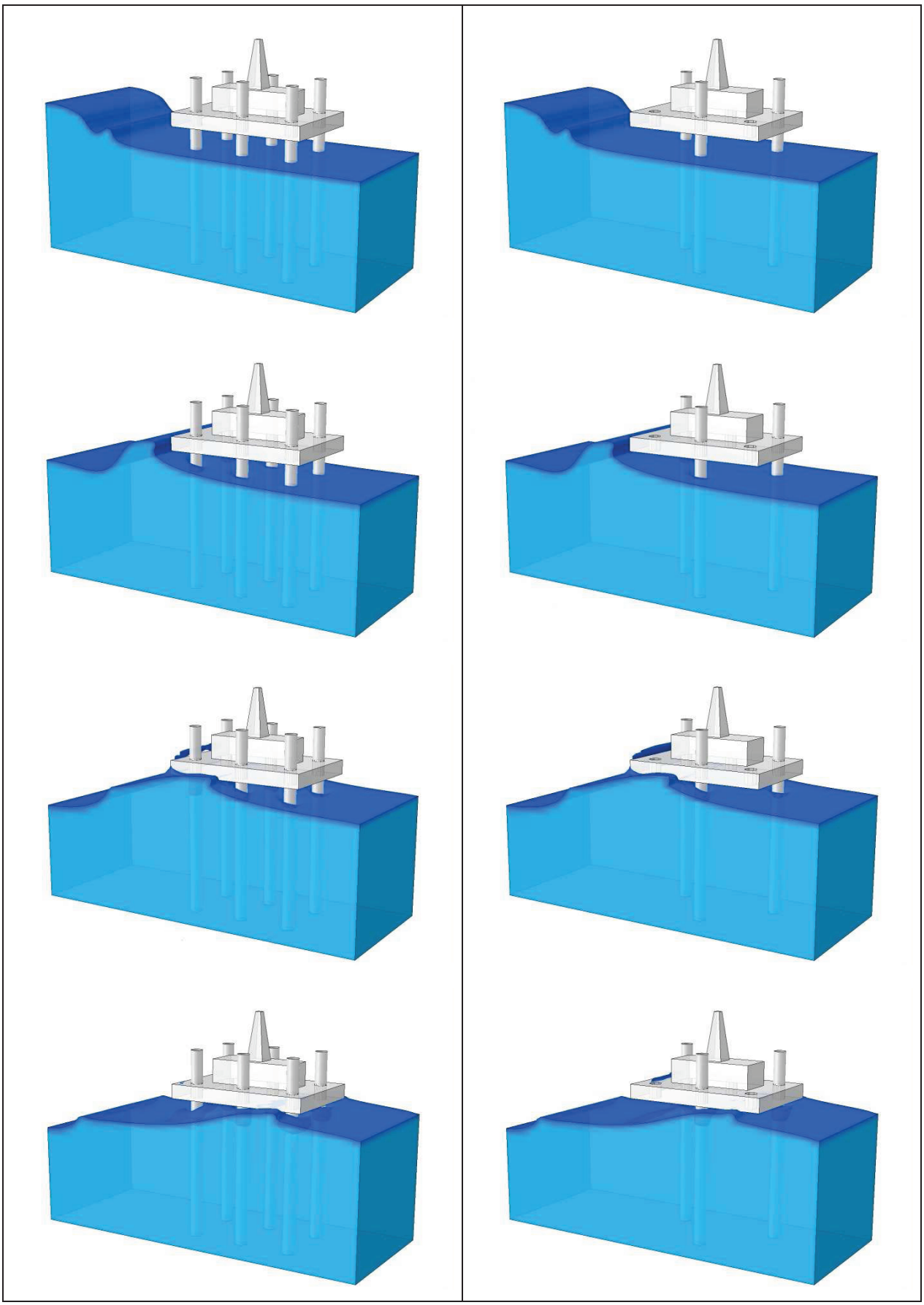

Figure 4: Assessment of structural redundancy for jack-up barges subjected to wave loading and tidal flows

The fluid flow is modelled in the Eulerian domain, where the combined actions of a design wave with height H = 10 m and an underlying fluid flow with velocity v = 1 m/s are imposed in an initial water depth d = 25 m. The constitutive behaviour of the water is specified with an equation of state, reducing the equations of motion to the Navier-Stokes equations for incompressible Newtonian fluids without bulk viscosity:

$$\rho\left(\frac{\partial \vec{v}}{\partial t} + \vec{v}\cdot\vec{\nabla}v\right) = -\vec{\nabla}p + \mu\nabla^2\vec{v} + \vec{f} \qquad \text{(Eq. 10)}$$

where ρ is the density, $\vec{v}$ the velocity field, p the pressure and μ the dynamic viscosity. Under the assumption of incompressible fluids, the density ρ is constant and the continuity of mass can be expressed as

$$\vec{\nabla}\cdot\vec{v} = 0 \qquad \text{(Eq. 10)}$$

Figure 4, the results of the CEL approach are presented for a jack-up barge subjected to tidal flow (v = 1 m/s) and wave loading (H = 10 m). Fluid-structure interaction is compared for a jack-up barge with six legs, and one with three legs. Although both designs can withstand the combined loading of waves and currents, the platform with six legs has a much higher stability. This is evident from Figure 5, where the transverse displacements of the top of the derrick are compared for both barges. The use of the CEL approach to evaluate structural redundancy for offshore platforms is presented in more detail in [3].

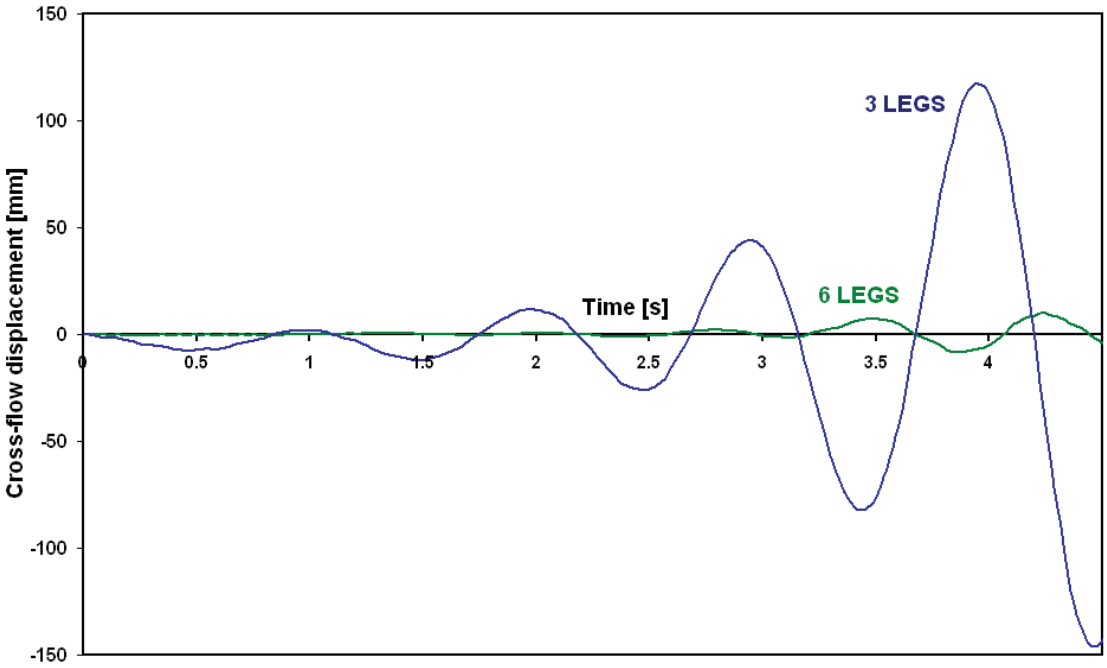

Figure 5: Cross-flow displacements of the derrick for both jack-up barges

Jack-up barges with four legs are commonly used, although the design with three legs has a wide application range as well. The latter one, however, has no structural redundancy, and is more vulnerable when operating in a disturbed sea state. While a mobile offshore structure like a jack-up barge is designed to operate within a certain tidal window, it may not be able to cope with a 100 year design wave, like shown on Figure 6. As a result, it is important to monitor the flow conditions, and interrupt operations if the environmental conditions dictate the need for evacuation.

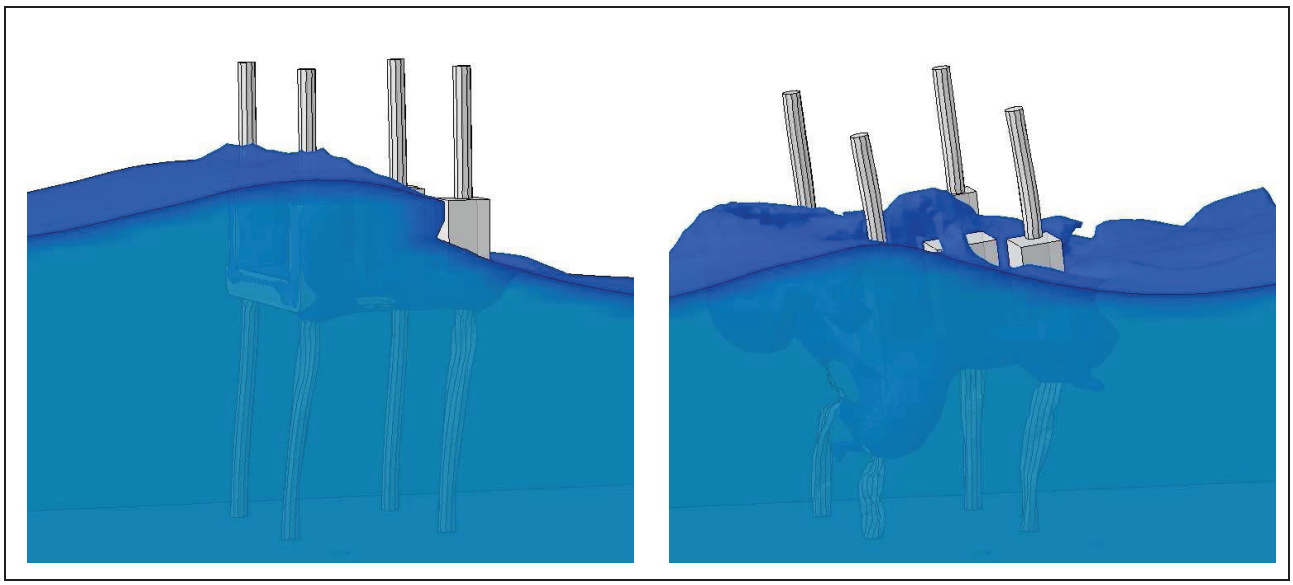

Figure 6: Collapse of the tubular legs when the jack-up barge is subjected to a 100 year design wave

3 FLUID STRUCTURE INTERACTION TO PREDICT VORTEX INDUCED VIBRATIONS

Vortex induced vibration (VIV) is a major cause of fatigue failure in submarine oil and gas pipelines [4] and steel catenary risers [5]. Even moderate currents can induce vortex shedding, alternately at the top and bottom of the tubular structure, at a rate determined by the flow velocity. Each time a vortex sheds, a force is generated in both the in-line and cross-flow direction, causing an oscillatory multi-mode vibration. This vortex induced vibration can give rise to fatigue damage of submarine pipeline spans and risers, especially in the vicinity of the girth welds. The huge financial loss associated with riser failure is an important incentive to develop more enhanced numerical tools to predict the VIV response of offshore structures [6].

Vortex shedding is governed by the Strouhal number

$$St = \frac{f_s D}{U} \qquad \text{(Eq. 11)}$$

where f_s is the vortex shedding frequency, D is the diameter of the riser (or pipeline) and U is the flow velocity. The Strouhal number is a function of the reynolds number

$$\mathrm{Re} = \frac{U D}{\upsilon} \qquad \text{(Eq. 12)}$$

which expresses the ratio of inertia forces to viscous forces, with the kinematic viscosity

$$\upsilon = \frac{\mu}{\rho} \qquad \text{(Eq. 13)}$$

as the ratio of the dynamic viscosity μ with the density ρ. A slender structure like a marine riser will start to oscillate in-line with the flow when the vortex shedding frequency

$$f_s \approx \frac{1}{3}\frac{\omega_0}{2\pi} \qquad \text{(Eq. 14)}$$

with ω_0 the lowest natural frequency of the riser, given by

$$\omega_0 = \frac{C}{L^2}\sqrt{\frac{EI}{m_e}} \quad \text{(Eq. 15)}$$

with C the end boundary coefficient, L the unsupported length, E the Young's modulus of the material, and

$$I = \frac{\pi}{64}\left(D_o^4 - D_i^4\right) \quad \text{(Eq. 16)}$$

the moment of inertia, where

$$D_i = D_0 - 2t \quad \text{(Eq. 17)}$$

is the inner diameter of the riser. The effective mass m_e includes the mass of the steel structure

$$m = \rho_{st}\frac{\pi}{4}\left(D_o^2 - D_i^2\right) = \rho_{st}\,\pi\left(D_o - t\right)t \quad \text{(Eq. 18)}$$

the internal fluid mass

$$m_i = \rho_i \frac{\pi D_i^2}{4} \quad \text{(Eq. 19)}$$

and the added mass

$$m_a = C_a\,\rho\frac{\pi D_o^2}{4} \quad \text{(Eq. 20)}$$

where the added mass coefficient C_a = 1 for vertical pipes and risers. On Figure 7, a Von Karman street in the wake of a marine riser is shown at the onset of turbulence. Each time a vortex sheds, a force is generated in both the in-line and cross-flow directions, causing an oscillatory multi-mode vibration. These oscillations can give rise to an '8-shaped' motion of the marine riser, which is detrimental to its fatigue resistance. A comprehensive review on vortex induced vibration is given in [7]. The implications of VIV on the design of marine risers are addressed in [8-10]. Details on fluid-structure interaction to predict flow induced oscillations in marine risers are given in [11]. In this paper, these modelling techniques are applied to study proximity effects of adjacent marine risers exhibiting wake interference.

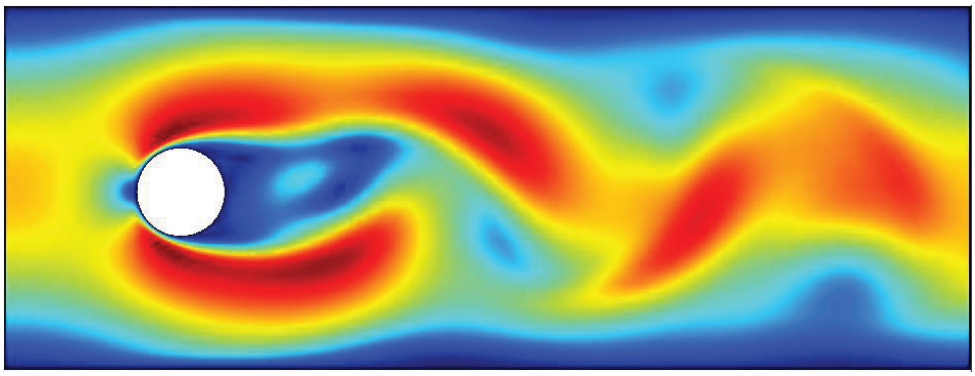

Figure 7: Von Karman vortex street in the wake of a marine riser

A careful review of flow interference between two circular cylinders in various arrangements has been presented by Zdravkovich [12], including an extensive list of references on this subject. Different studies for the tandem arrangement of two adjacent risers [13-16] have shown that the changes in drag, lift and vortex shedding are not continuous. Instead, an abrupt change for all flow characteristics is observed at a critical spacing between the risers.

It has been shown experimentally [13-16] that there is strong interference between two cylinders in tandem arrangement for spacing ratios with L/D < 3.5. At a spacing L/D ≈ 3.5, a sudden change of the flow pattern

in the gap between the adjacent risers is observed. A parametric CFD model [5] enables an easy and straightforward means to evaluate the influence of riser spacing. On Figure 8, flow patterns for different spacings L/D are shown, indeed endorsing the experimental observations of King [14], Zdravkovich [15] and Allen [17].

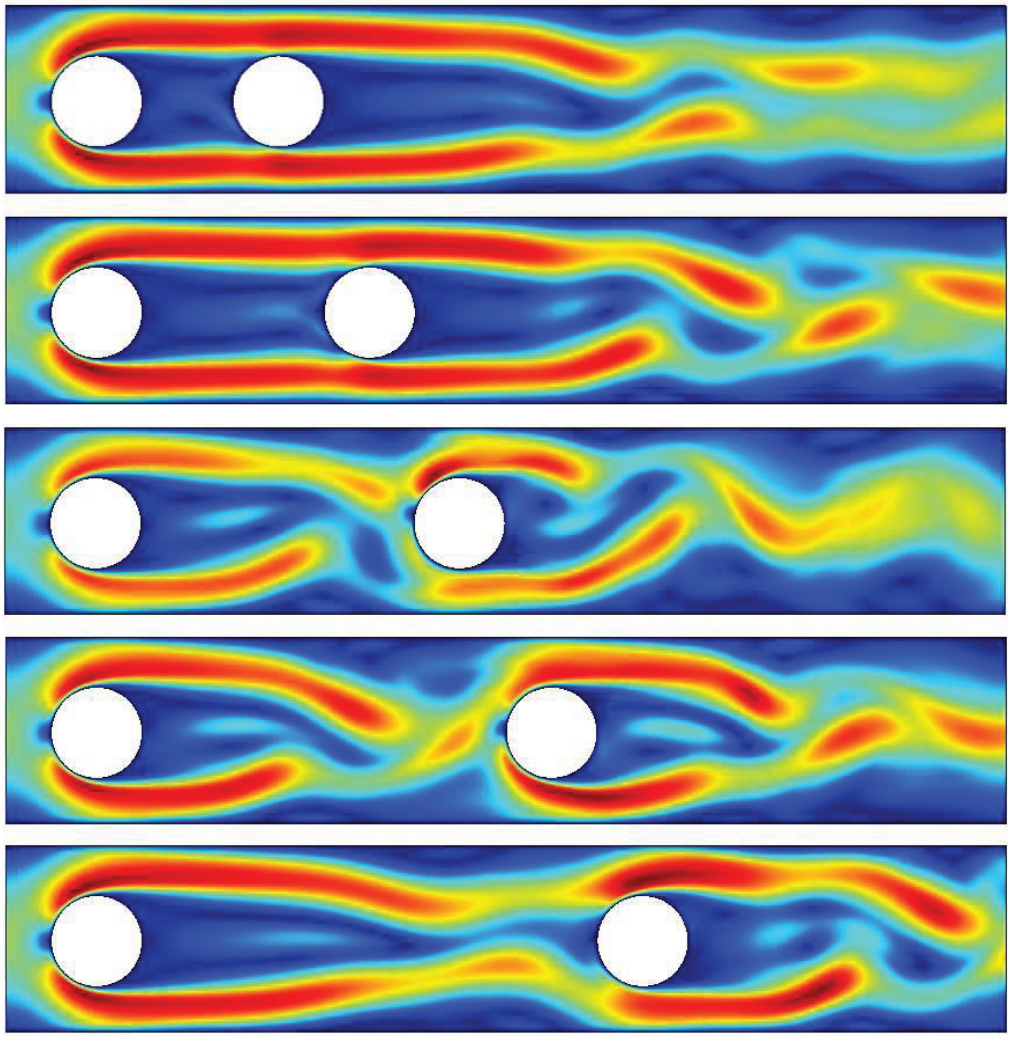

Figure 8: Flow patterns for different riser spacing L/D

Drag coefficient data [16-17] shows that the upstream cylinder takes the brunt of the burden, and that the downstream riser has little or no effect on the upstream one. For different values of spacing L/D, the drag coefficient

$$C_D = \frac{F_D(t)}{\frac{1}{2}\rho\langle U\rangle^2 D} \qquad \text{(Eq. 21)}$$

predicted by the CFD model is shown in Figure 9. Clearly, the drag coefficient on the upstream cylinder is not influenced by the downstream one, but a significant change in drag is observed on the downstream cylinder for L/D > 3.5.

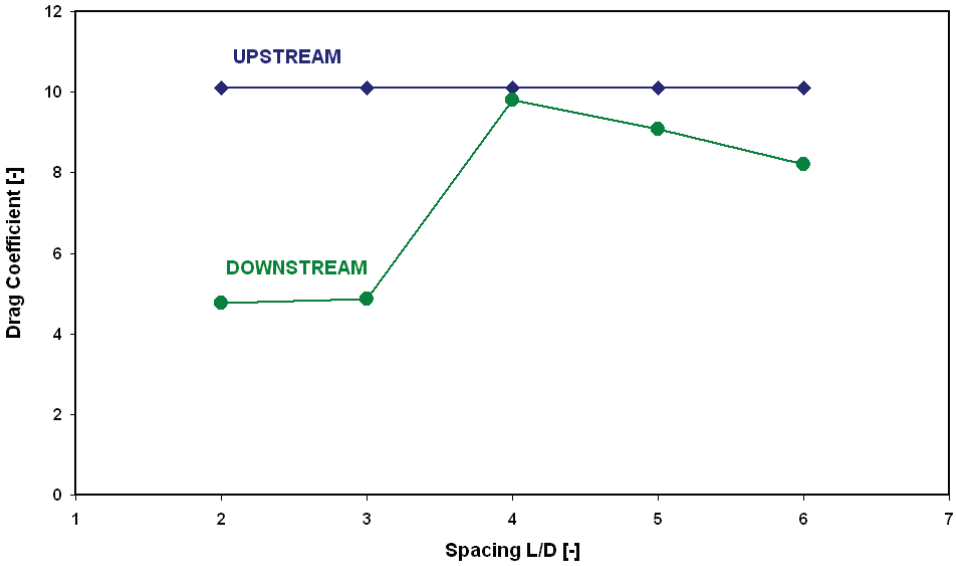

Figure 9: Predicted drag coefficients for twin risers in tandem arrangement

More details on proximity effects for risers in tandem arrangements at different flow directions can be found in [18]. Numerical simulations on multiple risers in tandem arrangements, risers in staggered arrangements and the application to platform legs are presented in [5] and [6].

4 STABILITY CONDITIONS FOR PARTIALLY BURIED SUBSEA PIPELINES

Subsea pipelines are installed on the seabed, and they are expected to stay in their installed position throughout their operational lifetime. As already indicated in the introduction, a subsea pipeline is subjected to environmental forces due to waves and currents, which may move the pipe and hence cause damage to its coatings or even overstressing the structure in case of excessive displacements. To ensure long term safe operation, pipelines are designed to be able under worst case conditions, and a concrete coating is applied to satisfy the stability conditions.

When assuming shallow water conditions, expressed by (Eq. 07), the horizontal water particle velocity and corresponding acceleration, induced by wave loading, is given by (Eq. 09). Moreover, a steady current can give rise to an additional fluid flow velocity (Eq. 02). Assuming that the waves are approaching the pipeline at an angle α and the current flow direction is at an angle β, the flow velocity will impose a lift force [19]

$$F_L = \frac{1}{2} C_L \rho D_o \left(u_x \cos\alpha + V \cos\beta\right)^2 \qquad \text{(Eq. 22)}$$

and a drag force

$$F_D = \frac{1}{2} C_D \rho D_o \left(u_x \cos\alpha + V \cos\beta\right)\left|u_x \cos\alpha + V \cos\beta\right| \qquad \text{(Eq. 23)}$$

where C_L and C_D are the lift and drag coefficients respectively, and D_o is the outer diameter of the pipe, including corrosion allowance, coating thickness and marine fouling. On top of that, the wave induced acceleration a_x gives rise to an inertia force

$$F_I = C_I \rho \frac{\pi D_o^2}{4} a_x \cos\alpha \qquad \text{(Eq. 24)}$$

with C_I the inertia coefficient. The empirical relations (Eq. 22) - (Eq. 24) are known as the Morison equations, relating the hydrodynamic forces (lift, drag and inertia) to the pipe diameter. On Figure 10, these forces are shown as a function of the phase angle θ, for a unit length of a pipeline with diameter D = 1 meter, subjected to a wave of height H = 10 meter and period T = 10 s and a steady current with velocity V = 0.5 m/s.

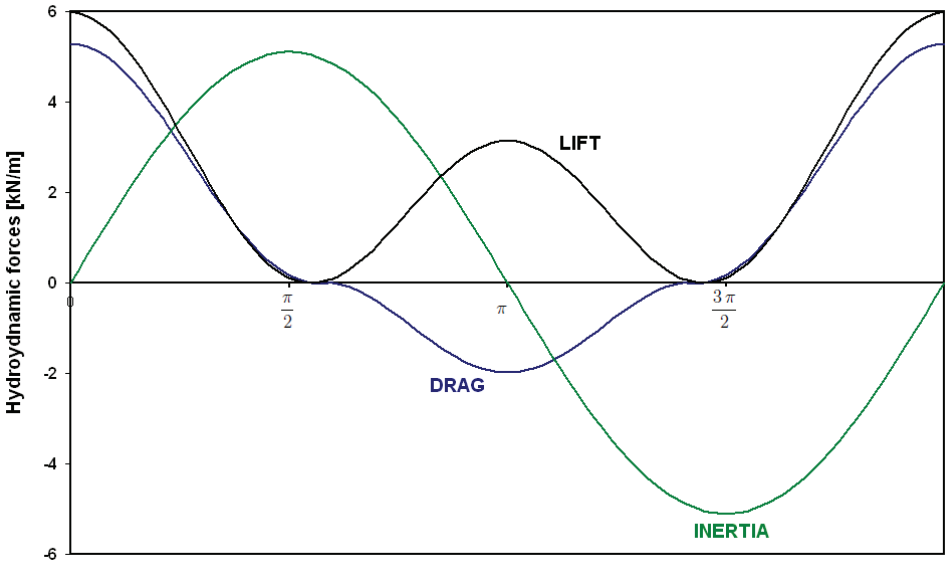

Figure 10: Hydrodynamic forces acting on a pipeline sitting on the seabed

The Morison's equations show that the drag and lift forces are proportional to the square of the fluid particle velocity, and that the inertia force is directly proportional to the fluid particle acceleration. The drag force acts in a direction parallel to the fluid flow, while the lift force is vertically upwards (i.e. normal to the seabed). The inertia force acts in the direction of the flow or against it, depending on whether the flow is accelerating or decelerating.

The Morison's equations are used to determine the appropriate thickness of a concrete weight coating to ensure offshore pipeline stability. The pipeline stability condition is considered to be satisfied when the forces that resist the pipeline displacement are greater than the forces that tend to displace it. The pipeline is stable when the submerged weight of the pipe w_p is greater than the lift force in vertical direction:

$$w_p = W - F_B \geq \lambda F_L \qquad \text{(Eq. 25)}$$

with W the weight of the pipe, coatings and contents, and F_B the buoyancy forces acting on the pipe. At the same time, the horizontal frictional force has to remain greater than the combined drag and inertia forces:

$$\mu\left(W - F_B - F_L\right) \geq \lambda\left(F_D + F_I\right) \qquad \text{(Eq. 26)}$$

where μ is the coefficient of friction between the pipe and the seabed. In the stability conditions (Eq. 25) and (Eq. 26), $\lambda = 1.1$ is a safety factor. Self-weight of the pipe (and its contents) is generally not sufficient to satisfy these criteria. In order to achieve stability, subsea pipelines are coated on the outside with high density concrete. The required thickness of the concrete coating is determined by an iterative procedure [#] such that the above criteria are satisfied for the most severe load combination, and for every value of the phase angle θ.

When the pipeline is sitting on the seabed, the hydrodynamic coefficients are frequently fixed to $C_D = 0.7$, $C_L = 0.9$ and $C_I = 3.29$. However, the hydrodynamic coefficients depend on both the Reynolds number (Eq. 12) and the Keulegan-Carpenter number [20]

$$KC = \frac{U\,T}{D} \qquad \text{(Eq. 27)}$$

In addition, the value for C_D, C_L and C_I is dependent on the position of the pipe. If the pipeline is sitting on the seabed –which is always intended by design- the hydrodynamic coefficients will be significantly different from those for pipeline spans with a gap between the pipe and the seabed, or for partially buried pipes. When the pipeline is trenched, the pipe weight must be higher than the lift forces induced by waves and currents in order to remain buried. As shown on Figure 11, the side slope will contribute to the horizontal stability.

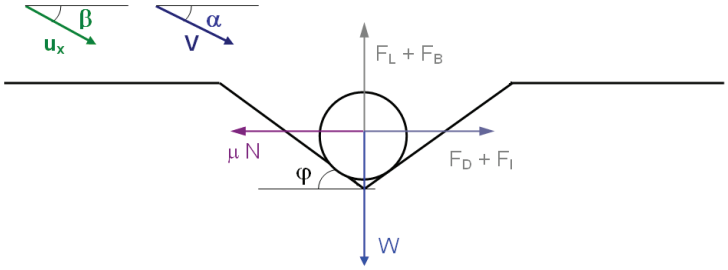

Figure 11: Stability conditions for a trenched offshore pipeline

The effect of the slope angle on the apparent pipe weight can be written as

$$\frac{W_t}{W_o} = \frac{1}{\cos\varphi + \frac{\sin\varphi}{\mu}} \qquad \text{(Eq. 28)}$$

Where W_t is the weight in the trench, and W_o the weight outside the trench. According to [#], the fluid flow velocity in the trench can be estimated as

$$\frac{V_t}{V_o} = 1 - 0.305\, d_t \qquad \text{(Eq. 29)}$$

with d_t the depth below the undisturbed seabed.

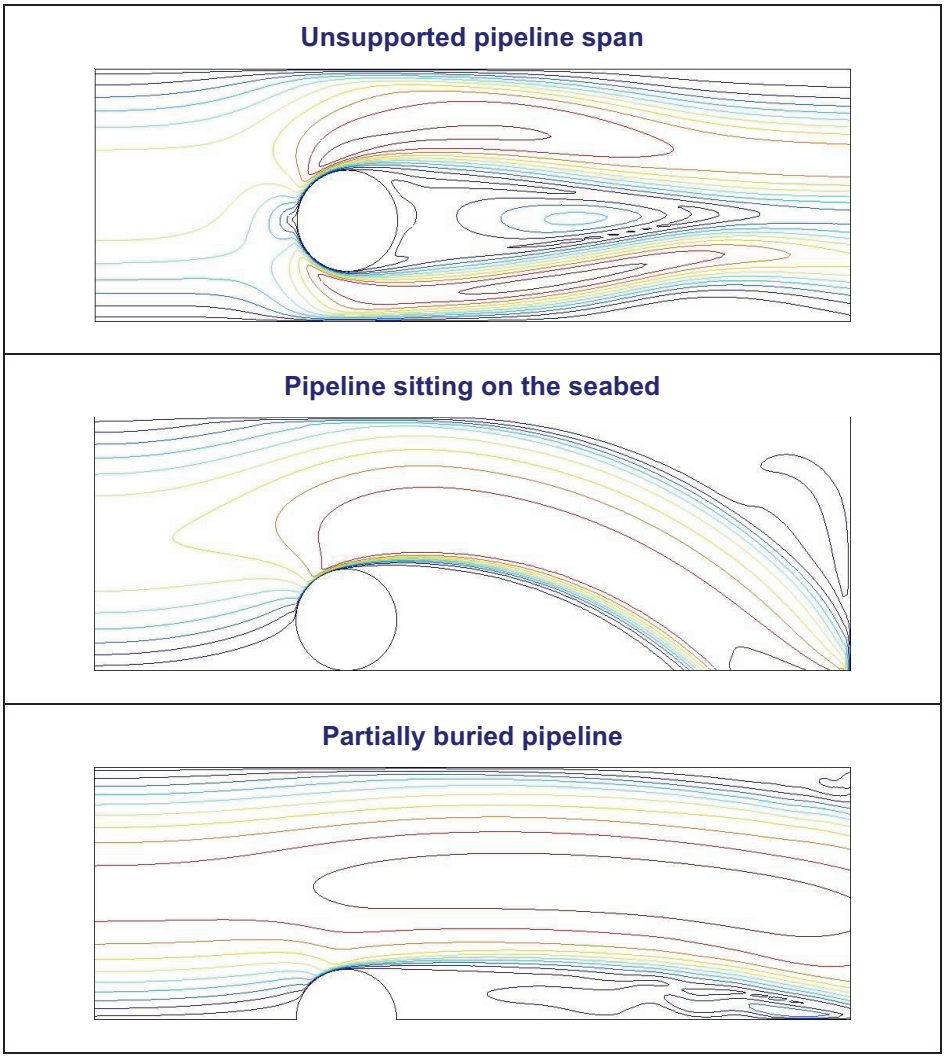

Figure 12: Fluid patterns for different pipe positions

A distinct difference between the flow patterns of a pipe sitting on the seabed, an unsupported pipeline span and a partially buried subsea pipe is observed from Figure 12. More details on boundary proximity effects and the evolution of the hydrodynamic forces can be found in [21].

5 CONCLUSIONS

In this paper, numerical tools and utilities to study the stability of offshore structures in shallow water depth were reviewed, and three case studies were presented:

1. The Coupled Eulerian Lagrangian (CEL) approach was demonstrated to combine the effects of fluid flow on the structural response of offshore structures. This approach was used to predict fluid flow around jack-up rigs, and to study to assess structural redundancy for different designs.
2. A computational fluid dynamics (CFD) analysis was performed to calculate the turbulent von Karman street in the wake of subsea structures. At higher Reynolds numbers, this turbulent flow can give rise to vortex shedding and hence cyclic loading. Simulations of fluid structure interaction were performed to reveal the effects of vortex induced vibrations for adjacent marine risers in tandem arrangements.
3. A hydrodynamic analysis was performed to evaluate the combined effects of steady current and oscillatory wave induced flow on partially buried subsea pipelines. The lift, drag and inertia forces are given by the Morison's equations, and a concrete weight coating is required to satisfy the stability conditions. It was shown that the values of the hydrodynamic coefficients depend on the Reynolds number, the Keulegan-Carpenter number and the position of the pipe relative to the seabed.

6 REFERENCES

[1] Sarpkaya T ; and Isaacson M., Mechanics of Wave Forces on Offshore Structures, 651 pp, 1981

[2] Wahab M.A., Finite Element Modelling of Several Physical Engineering Problems, Sustainable Construction and Design, Ghent, 2010

[3] Van den Abeele F. and Vande Voorde J., Coupled Eulerian Lagrangian Approach to Model Offshore Platform Movements in Strong Tidal Flows, Proceedings of the ASME 2011 30th International Conference on Ocean, Offshore and Arctic Engineering, OMAE2011-49639

[4] Van den Abeele F., Vande Voorde J. and Goes P., Numerical Modelling of Vortex Induced Vibrations in Submarine Pipelines, COMSOL Users' Conference Stuttgart, Germany, 2008

[5] Van den Abeele F. and Vande Voorde J., Flow Induced Oscillations of Marine Risers with Wake Interference, COMSOL Users' Conference Paris, France, 2010

[6] Van den Abeele F. and Vande Voorde J., Numerical Simulation of Multiple Marine Risers Exhibiting Wake Interference, Proceedings of the ASME 2011 30th International Conference on Ocean, Offshore and Arctic Engineering, OMAE2011-49639

[7] Gabbai R.D. and Benaroya H., An Overview of Modelling and Experiments of Vortex Induced Vibrations for Circular Cylinders, Journal of Sound and Vibration, vol. 282, pp. 575-616, 2005

[8] Ofougbu E.I., Review of Vortex Induced Vibration in Marine Risers, M.Sc. Thesis, Cranfield University, School of Applied Sciences, Offshore and Ocean Technology, 2008

[9] Ashiru A., Assessment of Vortex Induced Vibration Response in Higher Harmonics Mode, M.Sc. Thesis, Cranfield University, School of Applied Sciences, Offshore and Ocean Technology, 2007

[10] Shanks J.M., Static and Dynamic Analysis of Marine Pipelines and Risers, PhD Thesis, Cranfield Institute of Technology, College of Aeronautics, 1985

[11] Van den Abeele F., Vande Voorde J. and Goes P., Fluid Structure Interaction to Predict Fatigue Properties of Subsea Pipelines Subjected to Vortex Induced Vibrations, Proceedings of the 5th Pipeline Technology Conference, Ostend, Belgium, 2009

[12] Zdravkovich M.M., Review of Flow Interference between Two Circular Cylinders in Various Arrangements, Journal of Fluids Engineering, vol. 99(4), pp. 618-633, 1977

[13] Allen D.W. and Henning D.L., Vortex Induced Vibration Current Tank Tests of Two Equal Diameter Cylinders in Tandem, Journal of Fluids and Structures, vol. 17, pp. 767-781, 2003

[14] King R., Wake Interaction Experiments with Two Flexible Circular Cylinders in Flowing Water, Journal of Sound and Vibration, vol. 45(2), pp. 559-583, 1976

[15] Zdravkovich M.M., Flow Induced Oscillations of Two Interfering Circular Cylinders, Journal of Sound and Vibration, vol. 101(4), pp. 511-521, 1985

[16] Zhang H. and Melbourne W.H., Interference between Two Cylinders in Tandem in Turbulent Flow, Journal of Wind Engineering and Industrial Aerodynamics, vol. 41-44, pp. 589-600, 1992

[17] Allen D.W., Henning D.L. and Lee L., Riser Interference Tests on Flexible Tubulars at Prototype Reynolds Numbers, Proceedings of the Offshore Technology Conference, OTC-17290, 2005

[18] Mittal S. and Kumar V., Flow Induced Oscillations of Two Cylinders in Tandem and Staggered Arrangements, Journal of Fluids and Structures, vol. 15, pp. 717-736, 2001

[19] Mohitpour M., Golshan H. and Murray A., Pipeline Design and Construction, a Practical Approach, Third Edition, ASME, 2007

[20] Teh T.C., Palmer A.C., Bolton M.D. and Damgaard J.S., Stability of Submarine Pipelines on Liquefied Seabeds, Journal of Waterway, Port, Coastal and Ocean Engineering, ASCE, pp. 244-251, 2006

[21] Van den Abeele F. and Vande Voorde J., Stability of Offshore Pipelines in Close Proximity to the Seabed, Proceedings of the International Pipeline Technology Conference, Hannover, Germany, 2011